

Pump–probe photothermal spectroscopy using quantum cascade lasers

This article has been downloaded from IOPscience. Please scroll down to see the full text article.

2012 J. Phys. D: Appl. Phys. 45 125101

(<http://iopscience.iop.org/0022-3727/45/12/125101>)

View [the table of contents for this issue](#), or go to the [journal homepage](#) for more

Download details:

IP Address: 128.219.49.14

The article was downloaded on 08/03/2012 at 13:24

Please note that [terms and conditions apply](#).

Pump–probe photothermal spectroscopy using quantum cascade lasers

R H Farahi¹, A Passian^{1,2}, L Tetard¹ and T Thundat³

¹ Oak Ridge National Laboratory, Oak Ridge, TN 37831-6123, USA

² Department of Physics, University of Tennessee, Knoxville, TN 37996, USA

³ Chemical and Materials Engineering, University of Alberta, T6G 2V4 Edmonton, Canada

E-mail: passianan@ornl.gov

Received 14 November 2011, in final form 26 January 2012

Published 6 March 2012

Online at stacks.iop.org/JPhysD/45/125101

Abstract

Obtaining compositional information for objects from a distance remains a major challenge in chemical and biological sensing. Capitalizing on mid-infrared (IR) excitation of molecules by using quantum cascade lasers (QCLs) and invoking a pump–probe technique, we present a variation of the photothermal process that can provide spectral fingerprints of substances from a variable standoff distance. We have evaluated the modal variations of the QCL beam that must be taken into account when applying QCLs for photothermal measurements. The results compare well with spectra obtained from conventional IR spectroscopy. Guided by the results, the potential of the measurements to be extended such that each point within a target region may be spectrally interrogated to form a hyperspectral image is discussed.

(Some figures may appear in colour only in the online journal)

1. Introduction

Yielding spectroscopic information from the surface of objects at a distance requires remote excitation. Following such an excitation, collection of the ensuing radiation emitted by the molecules to be detected is particularly challenging due to scattering and interference with the substrate and the superstrate. While previous standoff studies have demonstrated the gathering of the radiation emitted as a result of direct scattering of the excitation photons [1], or the thermal emission [2], there exists a rich history of techniques based on photothermal spectroscopy (PTS) that may be able to obtain spectral information from a substance without the need to collect the scattered radiation. Using one or more probe beams, the resulting changes in thermo-physical and thermo-optic properties occurring at or near the site of the electromagnetic interaction of a pump beam may be monitored. One significant thermal effect that is monitored is the change in refractive index of both the sample and air near the absorption site [3–7], often raster-scanned in 1D or 2D to obtain thermal profiles across heterogeneous regions. Further observable effect is the spatial expansion due to the change in the thermal state of the material, where the volumetric changes expressed in the sample surface may be profiled [8].

Compositional analysis via vibrational spectra, such as the analysis of infrared (IR) absorption signatures, has been shown possible using variable wavelength pumps in early works of IR photoacoustic spectroscopy (PAS) [9–14]. IR PAS has been carried out using the tunable lines of the CO₂ laser (9.2–11.4 μm) [9, 11, 12] and dispersive or broad-band sources [10, 13, 14]. Given that a limitation in the PAS configuration is the sample requirement of close proximity or contact with the transducer, subsequent vibrational spectroscopy using non-contact photothermal methods have been developed. In this respect, to the best of our knowledge, only two configurations have been demonstrated: the mirage effect and photothermal deflection spectroscopy (PDS). In early work by Low *et al* in 1982, the mirage detection of the bending of a probe beam running orthogonal through the CO₂ beam was used to obtain absorption spectra of very low scattering “black” samples [4]. In an early demonstration of PDS by Reddy in 1983, the deflection of a probe beam through a transparent cell that was modulated by a dye laser beam was used for vibrational overtone spectroscopy to detect overtone transitions in benzene gas [5]. Although these PTS methods for vibrational spectroscopy continue to be used today, they are not scalable to remote analysis. Another common pump–probe PTS configuration where the probe beam is positioned nearly parallel to the pump [6, 7], and thus being scalable to

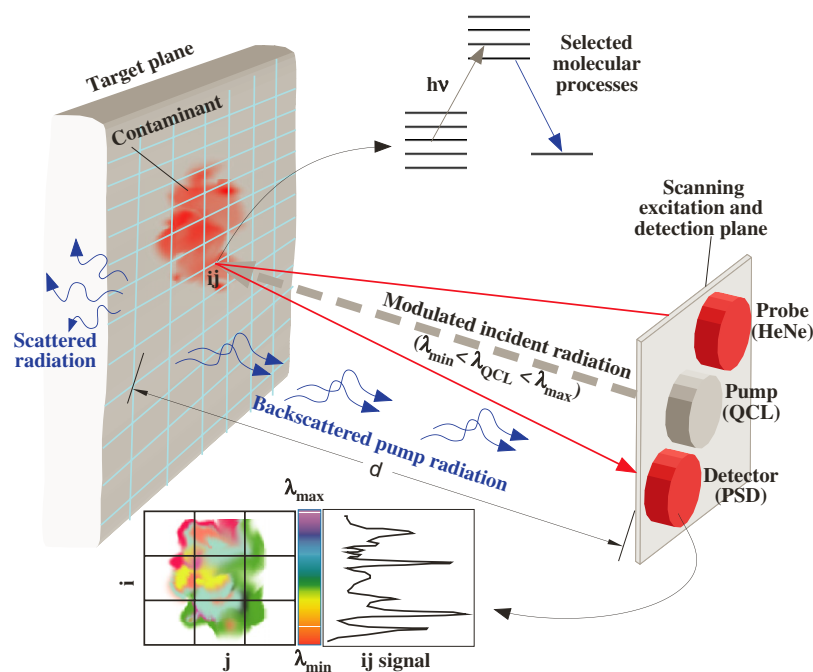


Figure 1. The concept of pump-probe standoff hyperspectral imaging using QCL-based photothermal spectroscopy of a target surface. The modulated QCL pump thermo-optically stimulates the surface via an available molecular channel. The minimally invasive probe beam (red) impinging on the same exposed surface location monitors the thermal response of the specimen, which yields the absorption spectra of the molecular composition of the target.

longer distances, had not been previously demonstrated for vibrational spectroscopy. Recent advancements in coherent IR sources such as the quantum cascade laser (QCL) [15] allow delivery of well-defined tunable beams in a precise range of wavelengths where IR absorption bands of interest reside. Thus, QCLs along with other IR lasers have become attractive IR sources for photothermal standoff detection of explosives and essentially employ two return-signal methods: thermal IR imaging and scattered IR radiation collection [16]. The thermal contrast of sample surfaces heated by QCLs with only selected absorption lines have been imaged with a thermal IR camera and interpreted for explosives identification [2]. In the radiation collection method, a continuous spectrum of scattered IR radiation from the QCL source was measured and compared with known absorption spectra of explosives [1]. However, employing the well-established pump-probe PTS configurations for the return signal in standoff applications have been absent. Furthermore, to our knowledge, the crucial consideration of the wavelength-dependent modal variations of the QCL beam in photothermal measurements has not been reported.

Similar to other remote sensing techniques such as radio detection and ranging (RADAR), and light detection and ranging (LIDAR), our QCL-based PTS requires a return signal, that is, a carrier of information of a characteristic property of the molecules to be detected. Using pulsed and/or continuous laser beams, a number of spectroscopic approaches have been attempted that provide vibrational and/or electronic information on the targeted molecules. For example, differential infrared absorption LIDAR (DIAL) [17, 18] or Raman scattering (RS) [19], provide signatures of the targeted chemicals via the vibrational spectra of the targeted molecules,

while other LIDAR-like spectroscopies such as laser-induced breakdown (LIBS) [20] or laser-induced fluorescence (LIF) [21], provide electronic spectra of the targeted molecules. Both LIBS and LIF are promising techniques to provide molecular information of the chemical composition (or the decomposition fragments) of the target material. In LIF spectroscopy the radiation associated with the spontaneous decay of photon-excited molecular states is detected, while in LIBS the target is laser-ablated into a plasma from which radiation is detected when excited electrons and ions decay into their ground states. In such cases, the adsorbed molecular film bound to the target surface will have to be vaporized by a laser beam.

In this paper, as shown in figure 1, we introduce a PTS technique scalable to long distances where a QCL pump and integrated laser probe system are able to detect the temperature induced changes in a target surface that are representative of the IR absorption spectra of the sample. The presented photothermal approach differs from previous work primarily in the following: (1) we demonstrate the application of vibrational spectroscopy using the PTS configuration where the pump and probe beams are nearly parallel; (2) we use probe beam reflectometry as the return signal in standoff applications thereby minimizing the need for expensive IR components such as cameras, telescopes and detectors; (3) we take into account the wavelength-dependent modal variations of the QCL pump source in the measured signal. Complex compounds such as cellulose, polystyrene, organophosphate pesticide, as well as common substances such as cosmetics and acrylic enamel paint were evaluated. The results suggest that chemical identification of remote substances through interpretation of their pump-probe PTS is a viable approach to standoff detection.

2. Experimental setup

The experimental configuration of the presented variation of PTS, shown in figure 1, employs a QCL pump (Daylight Solutions, Inc., Poway, CA) that delivers IR light to the target surface in the range 9.26–9.8 μm which is electronically tunable at a precision of 0.01 nm, 0.2 kHz, 0.02 μs pulse width and 1 mA. The thermal response of the sample was measured at 40 Hz. Electronically modulating the QCL at this low rate leads to low average pump power. To increase the average pump power, the QCL was modulated electronically to maximize its average output (100 kHz, 0.5 μs pulse width, 1000 mA). This rate is sufficiently high that the sample significantly only responds to the average power. Thus, an external (mechanical) chopper at 40 Hz further modulated the pump power incident on the sample to allow lock-in detection of the sample response.

The probe beam was delivered from a 5 mW 632.8 nm HeNe laser to the location of the thermal disturbance. A HeNe laser was used as the source of the probe beam primarily due to (1) well-defined Gaussian beam profile for focusing and controlling overlap with the pump beam, (2) power stability and the ease of power measurements and control, (3) availability of fast, accurate and compact detectors in the visible range and (4) lower absorption in the “fingerprint” part of the spectrum. The probe laser is reduced in power to less than 1 mW with a 1.0 neutral density filter so that thermal stimulation from the probe itself is minimal. The reflected probe beam is directed onto a segmented position sensitive detector (PSD) positioned 1 m away, where the major axis of probe deflection is recorded by lock-in detection at the pump modulation frequency. Thus the probe response is measured from the root mean square (rms) output of the lock-in, R , representing the probe beam variation read by the PSD. Since the modulation of R is a function of the overlap efficiency of the two laser beams’ projections onto the target sample plane, we examined the degree of overlap to within a fraction of a micrometre using the recently reported technique of remote detection of the optomechanical IR response of a multilayer gold coated silicon microcantilever (used as a detector here) [22].

As depicted in figure 1, considering a uniform Cartesian mesh over the region of interest $\Omega = \{\mathbf{r}(x, y, z) : x \in [x_l, x_r] \wedge y \in [y_l, y_b] \wedge z = \text{const.}\}$, we first note that each interrogated cell ij with the in-plane dimensions of $(\Delta x, \Delta y)$, may be characterized with two independent functions: (1) the topography $z = f(x, y)$ and (2) the spectral properties $s = g(x, y; \lambda)$ of the chemical content of the cell. The final map formed from the output of the PSD after a scan of Ω will therefore constitute a spatial convolution of f and g . Since in the presented technique, when the pump beam is absent, the probe beam can provide an estimate for f , then formally g may be obtained from the method of deconvolution. We therefore aim to study $s_{ij} = g(x_i, y_j; \lambda)$. For a thin layer of film with a thickness t and a known dielectric function ϵ on an arbitrary substrate with a dielectric function ϵ_s , the relative reflectivity r of the probe beam, incident at a small angle α in free space, can be readily calculated. For the

linearly polarized probe beam used, $r \propto \alpha, t, \text{Im}(\epsilon)$ (and also $\propto \text{Im}(1/\epsilon)$ for p polarization). Neglecting the minor potential (fixed) absorption of the probe beam, when the pump beam is absent, these parameters remain stationary. However, when the pump beam is turned on localized heating of the surface occurs. The pump heating leads to volumetric and thermo-optical changes of these parameters, which in turn alter the reflectivity. The pump radiation is absorbed according to the chemical composition of the film on the surface Ω , which is manifested by heating and thermal expansion of the surface. Thus a volumetric increase in the surface morphology is a consequence of an increase in absorption at a given wavelength.

Samples of glyphosate (Round-UpTM pesticide), purple cosmetic paint (Nail SavvyTM), α -cellulose (Sigma) dispersed in water, 0.72 μm latex spheres (Interfacial Dynamics Corp, Portland, OR) dispersed in water and black enamel paint (FolkArtTM enamel, Licorice) were chosen because of the availability of spectral absorption features in the range of the QCL. Cosmetic paint is primarily composed of nitrocellulose (cellulose nitrate) [23] and the enamel paint is acrylic-based. The samples were disposed and dried on n-type silicon (Si) wafer and aluminium (Al) substrates for pump–probe testing. The samples were also applied in the same manner on ZnSe slides or Si wafers for independent verification with a Fourier transform infrared (FTIR) spectrometer (Spectrum GX, Perkin Elmer) at a resolution of 4 cm^{-1} , an interval of 1 cm^{-1} and an optical path difference velocity (scan rate) of 0.2 cm/s . We experimentally found PTS step sizes of 4–10 nm to be adequate for comparison to the FTIR spectra, taking into account the resolution setting of the FTIR spectrometer. The FTIR evaluations were performed in transmission, thus the coatings were considered optically thin.

3. Results and discussion

In figure 2, the experimental results are plotted for raw R (blue), compensated R (black) and FTIR absorption spectra (red) of common substances. Compensated R accounts for the wavelength-dependent behaviour of the QCL power level which significantly alters the spectral signature of raw R . The power $P_L(\lambda)$ was measured by tuning the QCL over its entire wavelength range and monitoring the highly-sensitive, area-dependent deflection of a silicon microcantilever sensor that was placed in lieu of a sample surface, shown in the inset in figure 2(b), and subsequently was used to calculate compensated $R = R_{\text{raw}} P_L / \max(P_L)$. In figure 2(a), the PTS spectral signature of black enamel paint appears to have improved with compensation. In figure 2(c), the probe response of glyphosate pesticide partially catches a major absorption peak centred at 8938 nm corresponding to the contributions of the stretching of the alkyl group with a possible contribution from the amine substituent. Over the frequency range measured by the laser, the PTS signal dropped significantly as the wavelength increased, as was also observed in absorption measurements with the FTIR. The PTS response also appeared to improve with compensation for cosmetic paint, shown in figure 2(d). The spectrum of the cosmetic paint may partly originate from the absorption of the carbonyl

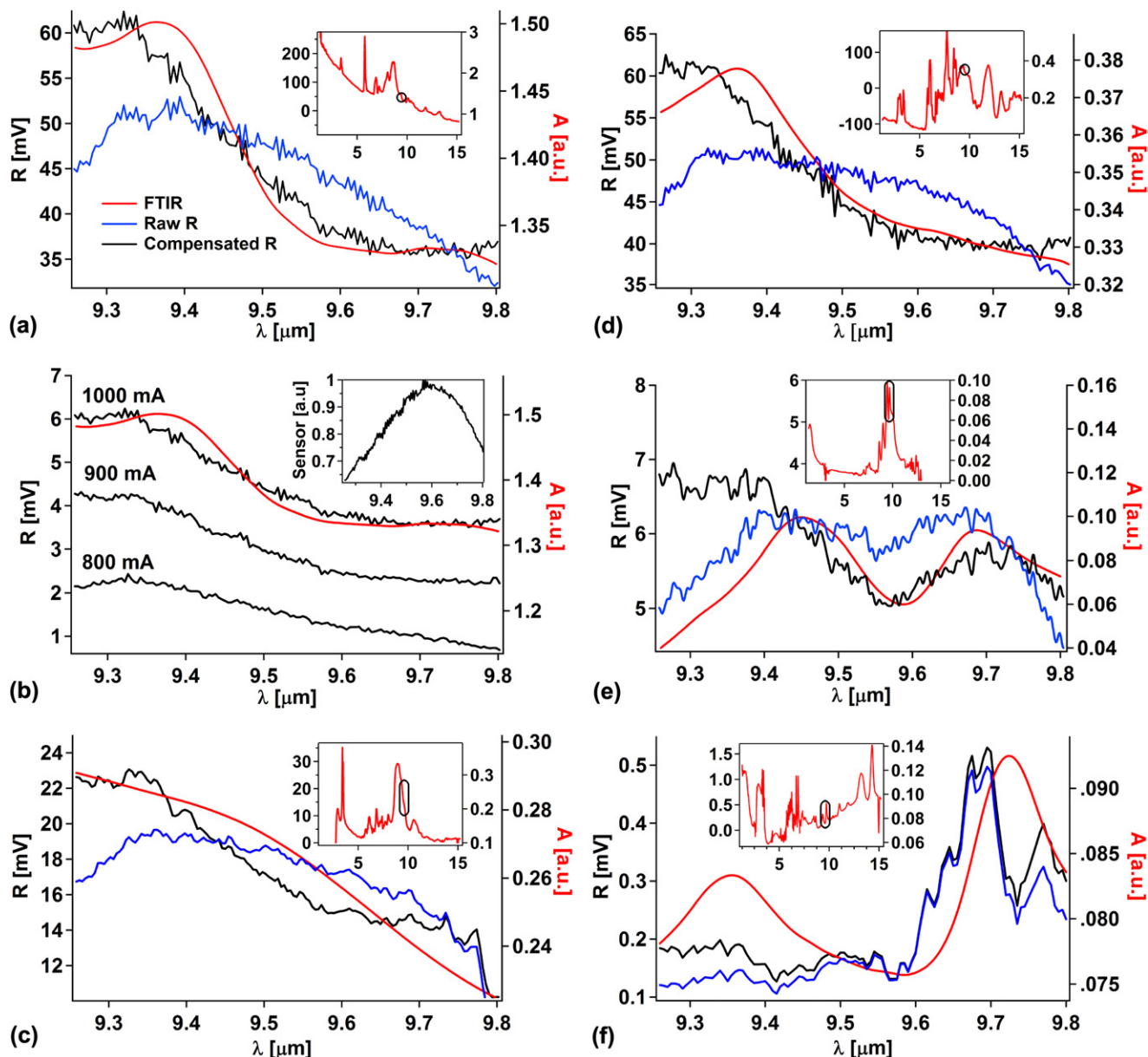


Figure 2. PTS probe responses, R , both raw (blue) and compensated (black), are compared with the FTIR absorption spectra (red) of common substances. The raw responses (blue) are compensated (black) for the wavelength-dependent power level of the QCL shown in the inset of (b). Broad FTIR spectra are plotted in the insets and marked where the QCL range occurs. (a) Black enamel paint on Al substrate. (b) Black enamel paint on Al substrate at QCL power levels 1000, 900 and 800 mA. (c) The pesticide glyphosate on Al substrate. (d) Purple cosmetic paint on Al substrate. (e) Insoluble α -cellulose crystals on Si substrate. (f) Latex spheres of 0.72 μm diameter on Si substrate.

group of the phenoxy group. For α -cellulose in figure 2(e) the compensation only partially improved the spectral signature and for polystyrene in figure 2(f) the compensation had a less dramatic effect. The appearance of a higher degree of noise for α -cellulose and polystyrene may be explained in part by the relatively low overall IR absorption which is responsible for generating the PTS signal. A perspective of where the PTS measurements took place within the broad FTIR absorption spectra of the substances is provided in the insets in figures 2(a),(c)–(f), where the corresponding inset axes units are the same as the major plot. It is noted that the maximum absorption peaks of the samples were not necessarily in the range of the QCL; however, the QCL-based PTS method was still capable of detecting subtle variations in absorption.

Some discrepancies between the QCL-based PTS and FTIR spectra were anticipated. While the FTIR spectra can be background corrected for ambient conditions such as H_2O and CO_2 , background correction of PTS remains a challenge. In interesting work by DeBellis and Low in 1988, the frequency-dependent phase lag in the photothermal signal was used to compensate possible effects of photothermal saturation, which improved the spectral signatures [24]. Possible saturation of the PTS signal was also investigated by analysing the effect of the overall QCL operating power level on the spectral curve. For example on black enamel paint in figure 2(b), the power level was changed by modifying the QCL current level (800, 900 and 1000 mA). As the operating power level was lowered the thermal response was reduced, however, in this

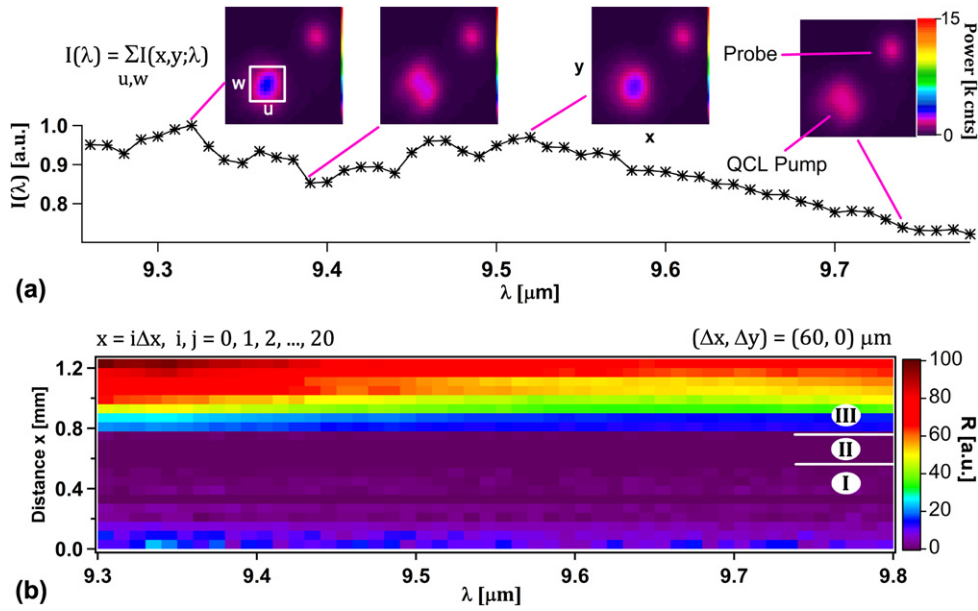


Figure 3. (a) The QCL energy $I(\lambda)$ and selected beam profiles revealing the QCL modes. The probe beam is offset for illustration purposes. (b) Spectra s_{ij} for a fixed j and $i = 1, 2, \dots, 20$ scanning over black enamel paint (I), Al substrate (II), purple cosmetic paint (III).

case the peak-to-valley ratio was retained. Further differences between FTIR and PTS spectra in our work were identified to be attributable to wavelength-dependent modal changes of QCL that emerge in the probe response R shown in figure 3(a). For each wavelength in the acquired spectra, the QCL beam near the focal distance was imaged with a beam profiler (Pyrocam III, Ophir Optonics) at a frame rate of 48 Hz. The beam profile was observed to markedly undergo intensity and shape variations as the wavelength was tuned. Representative profiles of the QCL beam (shown with the probe beam offset for visualization purposes) corresponding to selected wavelengths are displayed as inset images in figure 3(a). To quantify this effect, the sum of the beam intensity $I(\lambda)$ in an estimated area (u, w) that would overlap the probe beam is plotted. Another issue is the spatial overlap of the probe and pump beams. The overlap dependence on the probe response has been well documented by Aamodt and Murphy in 1981 [25]. Using the microcantilever sensor as described above, the pump-probe response over the range (current, wavelength, frequency) of the QCL was observed to be stable, thus we concluded that the spatial overlap stability was sufficient for our work. However, correction for additional variations that might occur from modal changes that could affect the spatial overlap of the two beams as a function of frequency should also be considered. A non-optimal overlap of a probe beam with a shape-invariant excitation source would result in an overall reduction in the probe signal [25]. However, a discernable overlap offset with the QCL beam could produce an unpredictable spectral probe response depending on where the overlap occurs due to modal shape variations.

The effects from the Al and Si substrates were considered for both the QCL and probe laser. The close to unity reflectivity of Al at both the QCL ($r \approx 0.98$) and the HeNe ($r \approx 0.9$) lines practically poses no spectral variation in the signal whereas in the case of Si with $0.57 \leq r \leq 0.615$ but negligible absorption in the QCL range, the significant absorption of

about 0.22 at the probe line can constitute a stationary thermal source that can cause low frequency fluctuations in the data. This fluctuation is clearly visible in both Si-based data shown in figure 2(e), (f). The absorption at the probe wavelength generates heat that propagates through the readout region, which, subject to conductive and convective thermal properties of the system including the surrounding air, can typically result in additional noise. In certain cases, the single wavelength of the low-power probe beam is expected to interact with the various sample-substrate systems. However, any potential minor thermal contribution of the probe is easily accounted for in our measurements. Similar considerations must be made for the reflectivity r of the substances at the probe wavelength. The total signal on the PSD is reduced when the light intensity of the probe is attenuated as a result of low reflectivity of the sample surface. For our samples, the black enamel paint and the purple cosmetic paint had the highest reflectivity, while the α -cellulose and polystyrene had the lowest reflectivity due to surface roughness. The α -cellulose and polystyrene samples were an aggregation of loosely-bound particles that produced high surface roughness, thus contributing to low reflection of the probe beam onto the PSD. The glyphosate pesticide sample was nearly transparent in the visible region, thus the probe response may be largely due to reflection off the underlying thermally expanded aluminium substrate from the IR absorption of the pesticide. This may explain why, although the QCL range encompassed a major absorption differential in the pesticide and should have yielded the highest signal, the probe response was less than that of the higher reflective paints. Furthermore, in our previous studies we have measured a nonlinear probe response from laser reflectometry on localized evolving curved surfaces of liquid [26]. In this PTS study, the confined thermal expansion of the surface also produces a similar volumetric effect, albeit much smaller. The effect of the nonlinearity would be to amplify the probe response as the

thermal expansion and associated curvature increase, which may be advantageous.

The QCL-based pump–probe analysis could be extended to a rastered system where a spectrum may be taken at each point to form a hyperspectral image. To this end, the substrates were mounted on a precision translation stage allowing 3D control of the sample surface with respect to the pump–probe system. As a demonstration of a potential for hyperspectral capability, a 10 nm resolution spectral interrogation (s_{ij}) at each point ($\Delta x = 60 \mu\text{m}$) of a 1.2 mm line scan across black enamel paint (0–0.48 mm), Al substrate (0.48–0.72 mm), and purple cosmetic paint (0.72–1.2 mm) is shown in figure 3(b). Topographic contributions within the same material ($\propto f$) were corrected using the sum signal of the PSD by assuming a height change would result in a partial probe deflection off of the PSD. While true hyperspectral imaging would process and sort spectroscopic information s_{ij} into color codes representing the various target chemicals, the preliminary result of a 1D scan clearly distinguishes the three surface regions through spectral signatures.

4. Conclusion

The non-contact detection of one or more dominant thermal effects due to response to an IR source allows compositional analysis of the sample via absorption spectroscopy. However, measurements of remote substances have unique challenges. Pump–probe PTS configurations which have demonstrated vibrational spectroscopy, such as mirage detection and PDS, where the pump and probe beams are transverse, are not scalable to measurements at longer distances. Pump–probe PTS configurations where the pump and probe beams are nearly parallel and are able to interrogate at distances have not previously employed vibrational spectroscopy. We have demonstrated QCL-based pump–probe vibrational spectroscopy that can be applied to standoff sensing without the use of elaborate IR cameras, telescopes or detectors in acquiring a return signal, as is the case with current scattered radiation collection and thermal IR imaging methods. We have analysed the power and beam profile of the QCL as a function of wavelength, which needs to be considered when interpreting the return signal. For cases where the molecular species, the substrate on which they are found, or the superstrates in which they reside exhibit strong absorption in the spectral part of interest, the presented technique can provide an important circumvention to the often difficult collection of weak IR emission. Based on the preliminary cell-by-cell measurements, our variation of PTS can be extended towards hyperspectral imaging. Common substances of organophosphate pesticide, paint, cosmetics, cellulose and polystyrene were evaluated by the QCL-based PTS technique and compared well with the reference FTIR spectra. The results are applicable to the standoff detection of a larger category of chemicals, as well as applications in other fields of research.

Acknowledgments

This research was sponsored by the laboratory directed research and development (LDRD) fund. ORNL is managed by UT-Battelle, LLC, for the US DOE under contract DE-AC05-00OR22725.

References

- [1] Van Neste C W, Senesac L R and T Thundat 2009 Standoff spectroscopy of surface adsorbed chemicals *Anal. Chem.* **81** 1952–6
- [2] Furstenberg R, Kendziora C A, Stepnowski J, Stepnowski S V, Rake M, Papantonakis M R, V Nguyen, Hubler G K and McGill R A 2008 Stand-off detection of trace explosives via resonant infrared photothermal imaging *Appl. Phys. Lett.* **93** 224103
- [3] Fang H L and Swofford R L 1979 Analysis of the thermal lensing effect for an optically thick sample—a revised model *J. Appl. Phys.* **50** 6609–15
- [4] Low M J D, Morterra C, Severdia A G and Lacroix M 1982 Infrared photothermal deflection spectroscopy for the study of surfaces *Appl. Surf. Sci.* **13** 429–40
- [5] Reddy K V 1983 Intracavity dye-laser photothermal deflection spectroscopy *Rev. Sci. Instrum.* **54** 422–4
- [6] Opsal J, Rosencwaig A and Willenborg D L 1983 Thermal-wave detection and thin-film thickness measurements with laser beam deflection *Appl. Opt.* **22** 3169–76
- [7] Rosencwaig A, Opsal J and Willenborg L D 1983 Thin-film thickness measurements with thermal waves *Appl. Phys. Lett.* **43** 166–8
- [8] Passian A, Lereu A L, Farahi H R, Ferrell L T and Thundat T 2007 *Thermoplasmonics in thin Metal Films Trends in Solid Film Research* (Hauppauge, NY: Nova Science Publishers)
- [9] Nordal P E and Kanstad S O 1977 Photoacoustic spectroscopy on ammonium sulphate and glucose powders and their aqueous solutions using a CO_2 laser *Opt. Commun.* **22** 185–9
- [10] Low M J D and Parodi G A 1978 Infrared photoacoustic spectra of surface species in 4000–2000 cm^{-1} region using a broad-band source *Spectrosc. Lett.* **11** 581–8
- [11] Kanstad S O and Nordal P E 1979 Infrared photoacoustic spectroscopy of solids and liquids *Infrared Phys.* **19** 413–22
- [12] Kanstad S O and Nordal P E 1980 Photoacoustic reflection-absorption spectroscopy (paras) for infrared analysis of surface species *Appl. Surf. Sci.* **5** 286–95
- [13] Low M J D and Parodi G A 1980 Infrared photoacoustic spectra of solids *Spectrosc. Lett.* **13** 151–8
- [14] Low M J D and Parodi G A 1980 Infrared photoacoustic spectroscopy of surfaces *J. Mol. Struct.* **61** 119–24
- [15] Faist J, F Capasso, Sivco D L, C Sirtori, Hutchinson A L and Cho A Y 1994 Quantum cascade laser *Science* **264** 553–6
- [16] Skvortsov L A and Maksimov E M 2010 Application of laser photothermal spectroscopy for standoff detection of trace explosive residues on surfaces *Quantum Electron.* **40** 565–78
- [17] National Research Council of the National Academies 2004 *Existing and Potential Standoff Explosives Detection Techniques* (Washington, DC: The National Academies Press)
- [18] Prasad C R, P Kabro and Mathur S L 1999 Tunable IR differential absorption LIDAR for remote sensing of chemicals *Proc. SPIE 3757 87 Application of Lidar to Current Atmospheric Topics III* ed A J Sedlacek and K W Fischer
- [19] Carter J C, Angel S M, M Lawrence-Snyder, Scaffidi J, Whipple R E, and Reynolds J G 2005 Standoff detection of high explosive materials at 50 meters in ambient light

- conditions using a small raman instrument *Appl. Spectrosc.* **59** 769
- [20] Bengtsson R, Grönlund R, Lundqvist R, Larsson A, Kröll S and Svanberg S 2006 Remote laser-induced breakdown spectroscopy for the detection and removal of salt on metal and polymeric surfaces *Appl. Spectrosc.* **60** 1188–91
- [21] Grönlund R, Lundqvist M, Larsson A, S Kröll and Svanberg S 2006 Remote imaging laser-induced breakdown spectroscopy and laser-induced fluorescence spectroscopy using nanosecond pulses from a mobile lidar system *Appl. Spectrosc.* **60** 853–9
- [22] Tetard L, Passian A, Farahi R H, Davison B H and Thundat T 2011 Optomechanical spectroscopy with broadband interferometric and quantum cascade laser sources *Opt. Lett.* **36** 3251–3
- [23] Toedt J, Koza D and K Van Cleef-Toedt 2005 *Chemical Composition of Everyday Products* (Westport, CT: Greenwood Press)
- [24] DeBellis A D and M J D Low 1988 Dispersive infrared phase angle photothermal beam deflection spectroscopy *Infrared Phys.* **28** 225–37
- [25] Aamodt L C and Murphy J C 1981 Photothermal measurements using a localized excitation source *J. Appl. Phys.* **52** 4903–14
- [26] Farahi R H, Passian A, Jones Y K, Tetard L, Lereu A L and Thundat T G 2009 Laser reflectometry of submegahertz liquid meniscus ringing *Opt. Lett.* **34** 3148–50